



New insights into water dynamics of Portland cement paste with nano-additives using quasielastic neutron scattering

Kunal Kupwade-Patil^{1,*} , Ali Bumajdad² , Craig M. Brown^{3,4} , Madhusudan Tyagi^{3,5} ,
Nicholas P. Butch^{3,6} , Abdullah F. Jamsheer² , and Oral Büyüköztürk^{1,*} 

¹Laboratory for Infrastructure Science and Sustainability (LISS), Department of Civil and Environmental Engineering, Massachusetts Institute of Technology, Cambridge, MA 02139, USA

²Nano-Science Group, Department of Chemistry, Faculty of Science, Kuwait University, Safat 13060, Kuwait

³NIST Center for Neutron Research (NCNR), National Institute of Standards and Technology, Gaithersburg, MD 20899, USA

⁴Department of Chemical and Biomolecular Engineering, University of Delaware, Newark, DE 19716, USA

⁵Department of Materials Science and Engineering, University of Maryland, College Park, MD 20742, USA

⁶Department of Physics, University of Maryland, College Park, MD 20742, USA

Received: 1 October 2018

Accepted: 29 November 2018

Published online:

7 December 2018

© Springer Science+Business Media, LLC, part of Springer Nature 2018

ABSTRACT

Early-age hydration kinetics of Portland cement with nano-additives such as nano-silica (NS) was examined using quasielastic neutron scattering (QENS). Cement pastes with different ratios of Portland cement to NS were prepared. The concentration of the NS played a major role in controlling the free and bound water during the hydration of the cement paste. Additionally, the effects of metakaolin (MK) with NS in Portland cements revealed that MK acts as a retarder by decreasing the bounding water capacity during the early age of hydration. An increase in the concentration of NS affected the degree of hydration by reducing the amount of free and mobile water in the gel pores when compared to Portland cement paste. Here, we show that the concentration of NS governs the early-age hydration process in Portland cements.

Introduction

The use of nano-additives like NS is becoming increasingly popular for developing durable, high-strength concretes and for repair applications [1–5]. However, limited research is available on understanding the early-age behavior when NS is used as a

supplementary cementitious material (SCM) or as an additive with Portland cements [2, 6–10]. Understanding the early-age behavior by using next-generation experimental capabilities is necessary to decipher the hydration mechanism in terms of water dynamics developed during the course of hydration [11]. By studying water dynamics during hydration,

Address correspondence to E-mail: kunalk@mit.edu; obuyuk@mit.edu

we can indirectly use this parameter to engineer nano-additives for specific applications in the cement and ceramics industry.

QENS is a powerful technique for accurately tracking the free and bound water during hydration to examine the effect of additives during the early course of cement hydration [12–15]. In comparison with NMR, the QENS and inelastic neutron scattering (INS) have superior measurement of timescales. The NMR data provide data in millisecond (10^{-3}) range, whereas QENS/INS reflect times in picosecond (10^{-12}) to femtosecond (10^{-15}) ranges [16]. These faster timescale measurements are necessary when SCMs are added to Portland cement for accelerating or retarding the rate of hydration reaction. Thus, QENS is effective in tracking the water dynamics in cement paste by accurately tracking the conversion of free to bound water during the course of hydration. The bulk water present during the early period of cement paste hydration is associated with the “free water,” while “restricted water” is attributed to the constrained water where the movement of the water is limited, as it is present inside the gel pores [12, 13, 16, 17].

To the best of our knowledge, the present work is the first to examine water dynamics using QENS on hydrating Portland cement with NS as the nano-additive. An initial understanding of the early age of hydration mechanism in Portland cement paste with 60-nm-sized NS was investigated using the parameters of bound water index (BWI) and by modeling QENS data for examining the freely diffusing and constrained water.

Materials and methods

Raw material characterization

The NS was prepared by implementing the sol-gel process [18] in the presence of polyoxyethylene monododecyl ether (Brij[®]35, Sigma-Aldrich). For the preparation of NS, 10.0 g of Brij[®]35 + ethanol solution (in 1:9 weight ratio) was added to 180 ml of ethanol and 20 ml of distilled water. Next, 3 ml of 30% solution of ammonia was added to this homogeneous mixture to catalyze the reaction followed by dropwise addition of 5.6 ml of tetraethyl orthosilicate (TEOS) with 1-h stirring. The resulting by-product was filtered, washed with ethanol, and separated

from the solution by centrifuging. The resultants were then heat-treated at 600 °C for 1 h. The average size of silica nanoparticles was found to be 60 ± 5 nm. Morphological features of silica NS along with detailed chemical composition can be found in Jamsheer et al. [2]. The final NS product was in a powder form and was mixed with Type I ordinary Portland cement (OPC). Furthermore, MK was used for one combination in addition to NS and Portland cement. MK is a common SCM used in the cement/ceramic industry and is a rich source of alumina and silica. Here, we examined the involvement of MK in NS during early age of hydration in Portland cement-based systems. The chemical composition was measured via X-ray fluorescence (XRF) for OPC and MK as shown in Table 1.

Mixing

Initial dry mixing of the NS/OPC and NS/MK/OPC was performed using a Daigger Vortex Genie 2 mixer (model no. G560) at 335 rad/s (3200 rpm). This mixing helped ensure that NS was uniformly mixed with the Portland cement prior to exposure to deionized water. For convention, we labeled each sample based on the binder and additive types. Therefore, a sample with 0.25%NS with 99.75 OPC is referred to as 0.25%NS, while the similar combination prepared with 2%NS, 8%MK, and 90% OPC is labeled as 2%NS8%MK (see Table 2). All samples were mixed with a constant water-to-cement ratio of 0.55 by mass. The samples were mixed near the experiment station and exposed to the neutron beam within 2 min of mixing.

Neutron scattering experiments

Experiments on cement pastes with NS and MK were conducted at room temperature on the disk chopper spectrometer (DCS) at the National Institute of Standards and Technology (NIST) Center for Neutron Research (NCNR) [19]. The incident monochromatic neutron wavelength was 6.0 Å, which results in an energy resolution of full width half maximum of about 64 μeV. The detectors were grouped to obtain a set of five spectra in the Q range from 0.42 to 1.47 Å⁻¹. An aluminum annular sample can of inner diameter of 17.8 mm and height of 110 mm were used. The pre-weighed cement paste (determined to provide 10% scattering and minimize effects of

Table 1 Chemical composition of OPC and MK

Binder type	Mass % as oxide									
	SiO ₂	Al ₂ O ₃	Na ₂ O	Fe ₂ O ₃	TiO ₂	K ₂ O	SO ₃	CaO	MgO	
OPC	16.73	3.63	0.34	3.28	0.24	0.62	3.92	62.27	1.22	
MK	51	44	< 0.05	< 2.20	< 3.0	< 0.4	< 0.5	< 0.2	< 0.1	

OPC ordinary Portland cement, MK metakaolin

Table 2 Composition of NS and MK additives

Sample	Weight percent (%)		
	OPC	NS	MK
OPC	100	0	0
0.25%NS	99.75	0.25	0
2%NS	98	2	0
2%NS8%MK	90	2	8

multiple scattering) was sandwiched in a thin aluminum foil, which was then rolled into an annulus having the same inner circumference of the cylindrical aluminum sample holder (diameter 17.5 mm). Sample height was about 90 mm (foil), with a beam mask of 80 mm × 17.5 mm. All the experiments were performed at an ambient temperature of 23 ± 0.2 °C as monitored using a Lakeshore temperature controller (accuracy 0.1 K).

The data reduction and modeling of the data were performed in the DAVE software environment [20]. The QENS spectrum, $S(Q, \omega)$, as a function of momentum transfer, Q , and energy transfer, ω , as measured by DCS were modeled using four components as shown in Eq. 1 [12, 14], comprising of a background term C_o , which is the fixed baseline intensity, and the terms of A and B . A is the scattered elastic intensity within the instrumental resolution that is associated with the chemically bound (CB) hydrogen atoms or also commonly known as “structural water” [12], B_1 is the number density of free hydrogen atoms as in the bulk water, Γ_1 is the Lorentzian half width at half maximum (HWHM) for the bulk water component, B_2 is the number density of hydrogen atoms in pseudo-bound or constrained form, Γ_2 is the second Lorentzian with the variable HWHM fitting parameter, and $R(Q, \omega)$ is the instrument resolution for which a vanadium standard was used.

$$S(Q, \omega) = C_o + \left(A\delta(\omega = 0) + B_1 \left[\frac{\Gamma_1}{\pi(\Gamma_1^2 + \omega^2)} \right] + B_2 \left[\frac{\Gamma_2}{\pi(\Gamma_2^2 + \omega^2)} \right] \right) \otimes R(Q, \omega) \quad (1)$$

From the above model, the bound water index (BWI) can be calculated which is the relative amount of immobile hydrogens and is determined by,

$$BWI = \frac{A + B_2}{A + B_1 + B_2} \quad (2)$$

where $A + B_2$ gives the total bound water in the hydrating paste. This three-component model allows three population of hydrogen [immobile hydrogen in cement paste (A), freely diffusing water (Γ_1), and constrained water (Γ_2)] in the cement paste to be tracked over the course of hydration as a function of time. The completely bound (CB) water is calculated by,

$$CB = \frac{A}{A + B_1 + B_2} \quad (3)$$

where A represents the immobile hydrogen or the number density of completely bound H atoms.

A sample fit using the three-component model of QENS data at $Q = 0.49 \text{ \AA}^{-1}$ obtained on 0.25%NS via DCS after 3 h of hydration is shown in Fig. 1. The data were averaged over each hour. The dotted gray line represents the elastic contribution by the Gaussian intensity, while the solid black line represents the total fit and the dashed lines represent the Lorentzian functions for modeling the data. We would like to clarify that even though two Lorentzians (free and pseudo-bound) are used to model the data and to calculate bound water index for the sake of discussion, in this study we are primarily concerned with free water Lorentzian which relates to the diffusion motion of the water molecules.

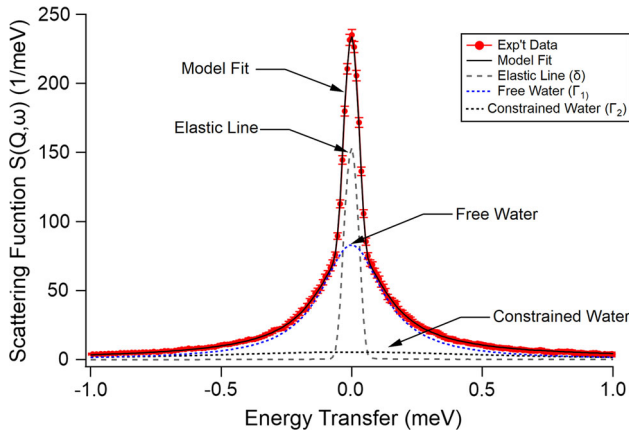


Figure 1 Typical fit of the QENS data after 1 h of hydration for cement paste prepared with NS and OPC. Details of instrument resolution (elastic line), double Lorentzian profile as dotted lines (black: constrained water; blue: free water).

Results and discussion

QENS

A three-dimensional plot of QENS data for 0.25%NS over 24 h is shown in Fig. 2a. Every hour data were summed over Q values centered at 0.42Å^{-1} , 0.50Å^{-1} , 0.60Å^{-1} , 0.70Å^{-1} , 0.80Å^{-1} , 0.90Å^{-1} , 1.00Å^{-1} , 1.10Å^{-1} , 1.20Å^{-1} , 1.30Å^{-1} , 1.40Å^{-1} , and 1.47Å^{-1} . Effect of hydration with time on the observed broadening is shown in Fig. 2b. Once the water interacts with the cementitious binder, the hydration reaction commences allowing the free water to convert to chemically bound water that represents the immobile state of water. A characteristic feature observed is the noticeable increase in the elastic intensity while simultaneously reducing the broadening of free water with the increase in hydration time. Previous studies have attributed the increase in elastic intensity to the formation of C–S–H phase along with crystalline phases of portlandite and ettringite [21–24]. Furthermore, once the cement paste starts to harden, then the minimal increase in elastic intensity is detected. However, the subtle mobility of water inside the cement paste is observed even among mature cement pastes; therefore, stabilization of elastic intensity cannot be used as a measure for determining the final setting time of cement paste [25].

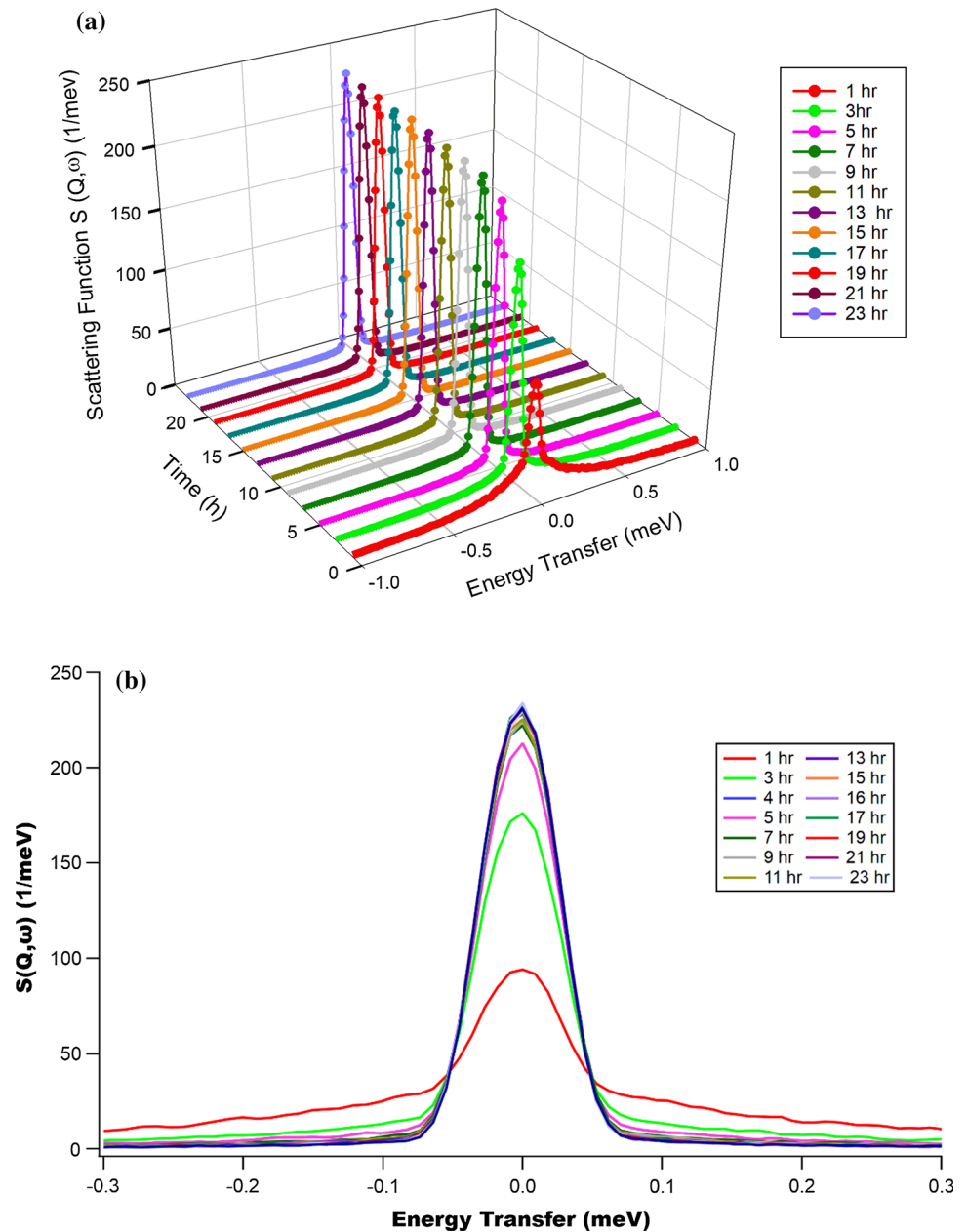
BWI is a common measure used for detecting the conversion of free to bound water in hydrating cement paste [12]. BWI values for all specimens over

24 h of hydration were extracted for all samples (OPC, 0.25%NS, 2.0%NS, and 2%NS8%MK) as shown in Fig. 3. The 24-h BWI plot is shown in Fig. 3a, and the magnified values for the first 4 h is shown in Fig. 3b. For each data point, 4 fifteen-minute scans were merged to obtain one BWI value. At all times of hydration, the 2%NS8%MK sample showed the least BWI as compared to the rest of the combinations. The 2%NS sample that exhibited a clear rise in BWI index from 0.71 to 0.76 was observed between the 3rd and 4th hour of hydration (refer to Fig. 3b). The BWI value for the 2%NS sample gradually increased to 0.9 after 24 h, while the rest of the samples stabilized to a BWI value of 0.75 as shown in Fig. 3a. This trend clearly indicates that the inclusion of 2%NS helps to increase the BWI by facilitating C–S–H and other related phases that may have contributed to the densification of the cement-based matrix.

As shown in Fig. 3a, most changes in BWI values were observed during the first 4 h of hydration as shown in Fig. 3b. A trend indicating the involvement of additives (SCMs) with Portland cement can clearly be observed after 1 h of hydration. The BWI data suggest that MK in combination with NS helps to retard the BWI values, while using only 2%NS can enhance the BWI value almost by a factor of ~ 1.5 . After 1 h of hydration, BWI values of 0.22, 0.28, 0.30, and 0.29 were calculated for 0.25%NS, 2%NS, OPC, and 2%NS8%MK, respectively.

As we decreased the dosage from 2.0 to 0.25% NS, the BWI value decreased from 0.77 to 0.72 at the 4th hour, implying the release of free water (refer to Fig. 3b). Here, a decrease in BWI indicates a higher availability of free water in the hydration process. In order to examine the immobile-hydrogen component, we evaluate the CB using Eq. 3. The CB values are calculated using Eq. 3 as shown in Fig. 3c. Here, CB signifies the consumption of free water in which C–S–H and calcium hydroxide product formation are overlaid on each other [14]. The BWI is comprised of the pseudo-bound component, which is associated with the available surface area governed by the formation of C–S–H gel [14]. By comparing BWI with CB, the BWI values are much higher than CB since BWI includes the pseudo-bound component that is associated with the available surface area dominated by C–S–H formation. Moreover, the elastic peak associated in the CB is readily discernible from the two Lorentzian components. The decrease in BWI and CB values for 0.25%NS was detected, while for

Figure 2 **a** Three-dimensional plot of QENS spectra for hydrating cement paste for 24 h at 0.55 water-to-cement ratio. The data were averaged over all Q values (0.42 \AA^{-1} , 0.50 \AA^{-1} , 0.60 \AA^{-1} , 0.70 \AA^{-1} , 0.80 \AA^{-1} , 0.90 \AA^{-1} , 1.00 \AA^{-1} , 1.10 \AA^{-1} , 1.20 \AA^{-1} , 1.30 \AA^{-1} , 1.40 \AA^{-1} , and 1.47 \AA^{-1}) and **b** two-dimensional plot exhibiting reduced broadening with the hydration time.



2%NS sample increased BWI and CB indicates a possibility of a “seeding effect,” which is commonly observed among cement pastes prepared with NS additives. The seeding effect is clearly influenced by the water dynamics, and it was observed as early as 3 h of hydration.

The BWI is affected by the formation of C–S–H gels, where during the initial course of hydration the free water is getting converted to bound water. Thus, examining the NS and MK dose effect by analyzing the HWHM obtained from the two Lorentzians is of essential value (see Fig. 4a, b). HWHM versus Q^2 for

freely diffusing and constrained water is shown in Fig. 4. In Fig. 4a, the free water Lorentzian (Γ_1) shows that the involvement of MK has the largest HWHM value in 2%NS8%MK as compared to the rest of the samples. Also, 2%NS sample had the smaller HWHM value for the freely diffusing water Lorentzian in contrast to the rest of the samples. Moreover, 0.25%NS had a slightly larger HWHM than OPC, while 2% NS had lower values than OPC. This result suggests that NS dosage is of importance and can be used for tailoring Portland cement pastes for controlling the free water dynamics.

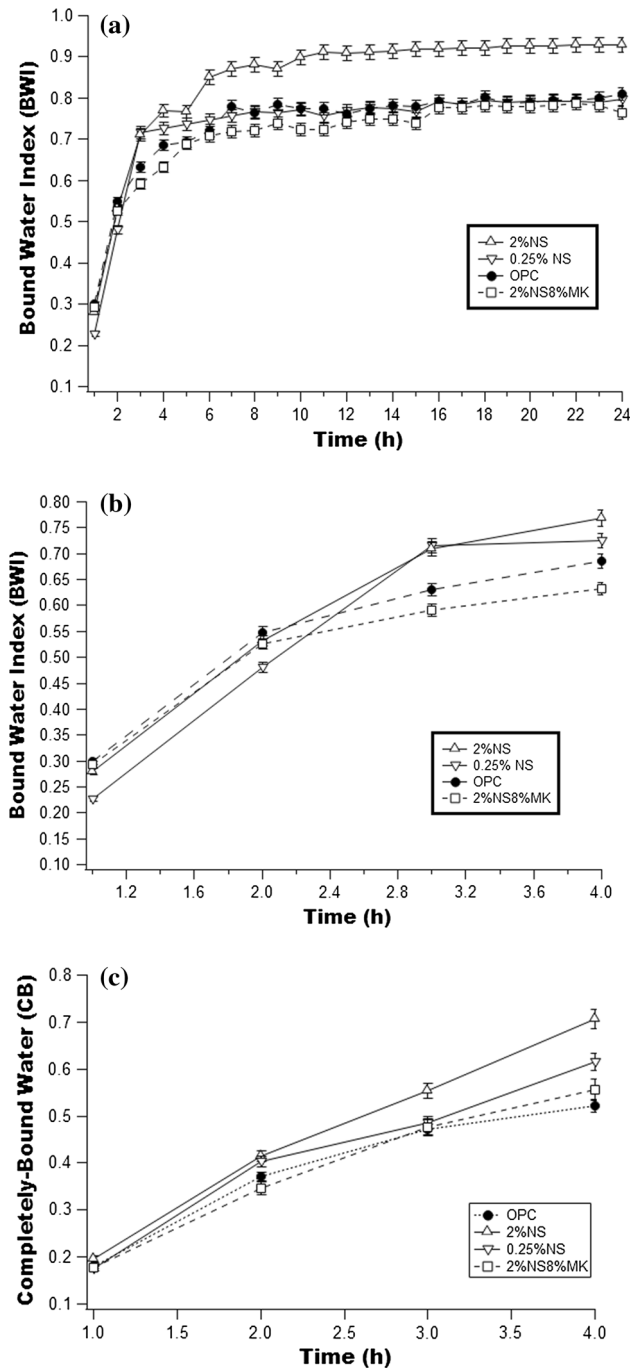


Figure 3 a Bound water index (BWI) over 24 h of hydration with Portland cement with NS and MK, b BWI for the first 4 h showing increase in BWI for 2%NS and decrease in 0.25%NS, c completely bound (CB) versus 4 h of hydration time.

The findings from this research show that cement paste prepared with 2%NS and OPC results in higher bound water and less free water when compared to Portland cement and 0.25%NS. In comparison with other combinations, inclusion of MK to OPC and

2%NS showed the presence of highest free water and less bound water. Thus, it is seen that careful consideration needs to be given when using SCMs or additives along with Portland cement. Specifically, water dynamics provides a direct measure of early strength gain, which is an essential requirement for structure-based concretes. For oil-well cementing under borehole conditions, retarders are used to inhibit the pozzolanic reaction to prevent setting and strength formation of cement pastes. In both cases, insight into motion of water is required to engineer the SCMs for specific applications. Therefore, early-age water dynamics in hydrating cement paste needs to be monitored carefully when using NS and MK, both of which are commonly used as accelerators/retarders for specific cement-based applications.

The current work was primarily focused on understanding the water dynamics in hydrating cement paste using QENS. Further studies using NMR would be beneficial for analyzing the mean chain lengths, while isothermal calorimetry will provide a direct insight into heat of hydration of the cement paste, respectively. Moreover, structural material analysis using neutron/X-ray pair distribution function (PDF), small-angle X-ray/neutron scattering (SAXS/SANS), synchrotron XRD, and wide-angle X-ray scattering (WAXS) would be valuable for deciphering the structural details related to microstructure development during hydration. Since we are dealing with disordered amorphous materials, neutron/X-ray PDF will provide access to the local structure of the material as opposed to long-range structure [26]. The primary advantage of the PDF technique is that it probes up to much higher real space ranges and detects all types of atoms. SAXS/SANS are useful techniques because they decipher the colloidal morphology of the cement paste by analyzing the size of the particles that occur in globules and fractals in irregular or fragmented shape during the hydration process [27]. The range of size by SANS-related techniques varies from nm to microns. WAXS is essential for detecting the phases during the hydration of cement pastes [27]. Thus, combining QENS with WAXS will provide both the water dynamics and the resulting micro-/nano-structural phases that evolves during the cement hydration process.

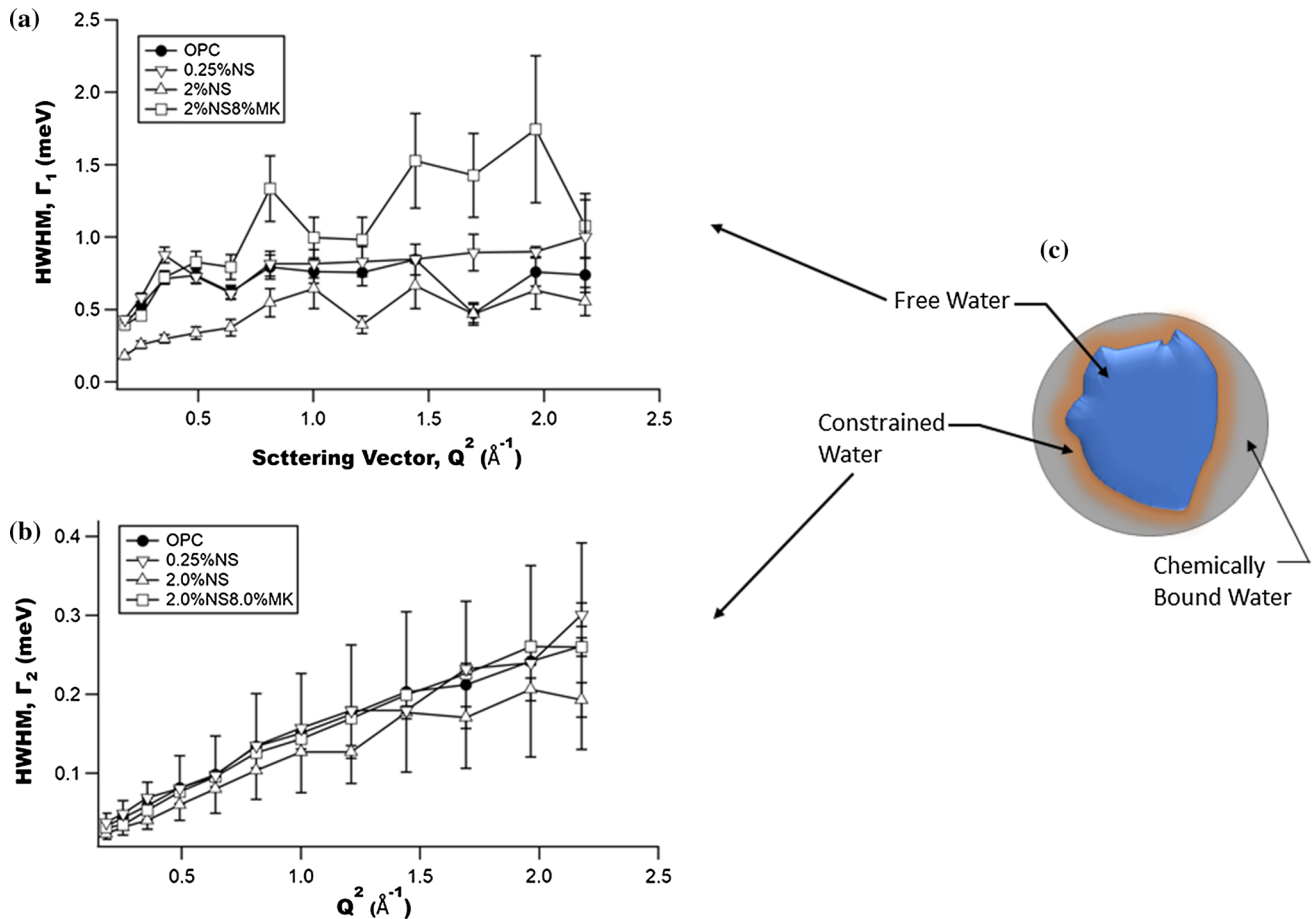


Figure 4 Half width half maximum (HWHM) from the Lorentzian on (a), freely diffusing water (Γ_1), (b) and constrained water (Γ_2) after 1 h of hydration.

Conclusions

This work shows that QENS can be used as a powerful tool for examining the influence and involvement of nano- and micro-sized additives for developing engineered cement pastes. To our knowledge, the current work is the first kind of study to use QENS technique to examine the effect of NS and MK in Portland cement pastes. The cement paste mixtures prepared with the combination of MK and NS showed a higher quantity of free water, while only NS with Portland cement paste had less free water and a higher bounding capacity to form constricted water. This work clearly shows that NS is a beneficial additive for accelerating early-age hydration, while careful consideration needs to be given to the dosage of NS as it can influence bounding capacity of water while possibly controlling the seeding effect in Portland cement-based systems. QENS technique can clearly detect the efficiency of

involvement of SCMs even at an early age of hydration. Thus, QENS can be an effective method for engineering retarders and accelerators for specific cement- and ceramic-based applications.

Acknowledgements

We thank the “Kuwait Foundation for the Advancement of Sciences” and “Kuwait-MIT Center for Natural Resources and the Environment” for their support during this work. The identification of any commercial product or trade name does not imply endorsement or recommendation by the National Institute of Standards and Technology (NIST). We acknowledge fruitful discussions with Dr. Andrew Allen from NIST.

References

- [1] Sobolev K, Lin Z, Flores-Vivian I, Pradoto R (2016) Nano-engineered cements with enhanced mechanical performance. *J Am Ceram Soc* 99(2):564–572. <https://doi.org/10.1111/jace.13819>
- [2] Jamsheer AF, Kupwade-Patil K, Büyüköztürk O, Bumajdad A (2018) Analysis of engineered cement paste using silica nanoparticles and metakaolin using ^{29}Si NMR, water adsorption and synchrotron X-ray Diffraction. *Constr Build Mater* 180:698–709. <https://doi.org/10.1016/j.conbuildmat.2018.05.272>
- [3] Brzozowski P, Horszczaruk E, Hrabciuk K (2017) The influence of natural and nano-additives on early strength of cement mortars. *Procedia Eng* 172:127–134. <https://doi.org/10.1016/j.proeng.2017.02.034>
- [4] Shah SP, Hou P, Konsta-Gdoutos MS (2016) Nano-modification of cementitious material: toward a stronger and durable concrete. *J Sustain Cem-Based Mater* 5(1–2):1–22. <https://doi.org/10.1080/21650373.2015.1086286>
- [5] Kupwade-Patil K, Cardenas H (2013) Electrokinetic nanoparticle treatment for corrosion remediation on simulated reinforced bridge deck. *J Nanopart Res* 15(9):1–16. <https://doi.org/10.1007/s11051-013-1952-3>
- [6] Senff L, Labrincha JA, Ferreira VM, Hotza D, Repette WL (2009) Effect of nano-silica on rheology and fresh properties of cement pastes and mortars. *Constr Build Mater* 23(7):2487–2491. <https://doi.org/10.1016/j.conbuildmat.2009.02.005>
- [7] Madani H, Bagheri A, Parhizkar T (2012) The pozzolanic reactivity of monodispersed nanosilica hydrosols and their influence on the hydration characteristics of Portland cement. *Cem Concr Res* 42(12):1563–1570. <https://doi.org/10.1016/j.cemconres.2012.09.004>
- [8] Singh LP, Zhu W, Howind T, Sharma U (2017) Quantification and characterization of C–S–H in silica nanoparticles incorporated cementitious system. *Cement Concr Compos* 79:106–116. <https://doi.org/10.1016/j.cemconcomp.2017.02.004>
- [9] Singh LP, Bhattacharyya SK, Shah SP, Mishra G, Ahalawat S, Sharma U (2015) Studies on early stage hydration of tricalcium silicate incorporating silica nanoparticles: Part I. *Constr Build Mater* 74:278–286. <https://doi.org/10.1016/j.conbuildmat.2014.08.046>
- [10] Singh LP, Bhattacharyya SK, Shah SP, Mishra G, Sharma U (2016) Studies on early stage hydration of tricalcium silicate incorporating silica nanoparticles: part II. *Constr Build Mater* 102:943–949. <https://doi.org/10.1016/j.conbuildmat.2015.05.084>
- [11] Biernacki JJ, Bullard JW, Sant G, Brown K, Glasser Fredrik P, Jones S, Ley T, Livingston R, Nicoleau L, Olek J, Sanchez F, Shahsavari R, Stutzman PE, Sobolev K, Prater T (2017) Cements in the 21st century: challenges, perspectives, and opportunities. *J Am Ceram Soc* 100(7):2746–2773. <https://doi.org/10.1111/jace.14948>
- [12] Thomas JJ, FitzGerald SA, Neumann DA, Livingston RA (2001) State of water in hydrating tricalcium silicate and portland cement pastes as measured by quasi-elastic neutron scattering. *J Am Ceram Soc* 84(8):1811–1816. <https://doi.org/10.1111/j.1151-2916.2001.tb00919.x>
- [13] Kupwade-Patil K, Tyagi M, Brown CM, Büyüköztürk O (2016) Water dynamics in cement paste at early age prepared with pozzolanic volcanic ash and Ordinary Portland Cement using quasielastic neutron scattering. *Cem Concr Res* 86:55–62. <https://doi.org/10.1016/j.cemconres.2016.04.011>
- [14] Allen AJ, McLaughlin JC, Neumann DA, Livingston RA (2004) In situ quasi-elastic scattering characterization of particle size effects on the hydration of tricalcium silicate. *J Mater Res* 19(11):3242–3254. <https://doi.org/10.1557/JMR.2004.0415>
- [15] Bordallo HN, Aldridge LP, Fouquet P, Pardo LC, Unruh T, Wuttke J, Yokaichiya F (2009) Hindered water motions in hardened cement pastes investigated over broad time and length scales. *ACS Appl Mater Interfaces* 1(10):2154–2162. <https://doi.org/10.1021/am900332n>
- [16] Peterson V (2010) Studying the hydration of cement systems in real-time using quasielastic and inelastic neutron scattering. In: Eckold G, Schober H, Nagler SE (eds) *Studying kinetics with neutrons*, Springer series in solid-state sciences, vol 161. Springer, Berlin, pp 19–75. https://doi.org/10.1007/978-3-642-03309-4_2
- [17] Kupwade-Patil K, Diallo SO, Hossain DZ, Islam MR, Allouche EN (2016) Investigation of activation kinetics in geopolymer paste using quasielastic neutron scattering. *Constr Build Mater* 120:181–188. <https://doi.org/10.1016/j.conbuildmat.2016.05.104>
- [18] Duran A, Serna C, Fornes V, Fernandez Navarro JM (1986) Structural considerations about SiO_2 glasses prepared by sol-gel. *J Non-Cryst Solids* 82(1):69–77. [https://doi.org/10.1016/0022-3093\(86\)90112-2](https://doi.org/10.1016/0022-3093(86)90112-2)
- [19] Meyer A, Dimeo RM, Gehring PM, Neumann DA (2003) The high-flux backscattering spectrometer at the NIST Center for Neutron Research. *Rev Sci Instrum* 74(5):2759–2777. <https://doi.org/10.1063/1.1568557>
- [20] Azuah RT, Kneller LR, Qiu Y, Tregenna-Piggott PLW, Brown CM, Copley JRD, Dimeo RM (2009) DAVE: a comprehensive software suite for the reduction, visualization, and analysis of low energy neutron spectroscopic data. *J Res Nat Inst Stand Technol* 114(6):341–358

- [21] Berliner R, Popovici M, Herwig K, Jennings HM, Thomas J (1997) Neutron scattering studies of hydrating cement pastes. *Physica B* 241–243:1237–1239. [https://doi.org/10.1016/S0921-4526\(97\)00819-3](https://doi.org/10.1016/S0921-4526(97)00819-3)
- [22] Berliner R, Popovici M, Herwig KW, Berliner M, Jennings HM, Thomas JJ (1998) Quasielastic neutron scattering study of the effect of water-to-cement ratio on the hydration kinetics of tricalcium silicate. *Cem Concr Res* 28(2):231–243. [https://doi.org/10.1016/S0008-8846\(97\)00260-3](https://doi.org/10.1016/S0008-8846(97)00260-3)
- [23] Peterson VK, Brown CM, Livingston RA (2006) Quasielastic and inelastic neutron scattering study of the hydration of monoclinic and triclinic tricalcium silicate. *Chem Phys* 326(2–3):381–389. <https://doi.org/10.1016/j.chemphys.2006.02.016>
- [24] Peterson VK, Neumann DA, Livingston RA (2005) Hydration of tricalcium and dicalcium silicate mixtures studied using quasielastic neutron scattering. *J Phys Chem B* 109(30):14449–14453. <https://doi.org/10.1021/jp052147o>
- [25] Bordallo HN, Aldridge LP, Desmedt A (2006) Water dynamics in hardened ordinary portland cement paste or concrete: from quasielastic neutron scattering. *J Phys Chem B* 110(36):17966–17976. <https://doi.org/10.1021/jp062922f>
- [26] Egami T, Billinge SJL (2012) *Underneath the Bragg peaks: structural analysis of complex materials*. Elsevier Science, Amsterdam
- [27] Kupwade-Patil K, Chin S, Ilavsky J, Andrews RN, Bumajdad A, Büyüköztürk O (2018) Hydration kinetics and morphology of cement pastes with pozzolanic volcanic ash studied via synchrotron-based techniques. *J Mater Sci* 53(3):1743–1757. <https://doi.org/10.1007/s10853-017-1659-4>